#### **REVIEW**



## Environmental sources of radio frequency noise: potential impacts on magnetoreception

Jesse Granger<sup>1</sup> · Steven A. Cummer<sup>2</sup> · Kenneth J. Lohmann<sup>3</sup> · Sönke Johnsen<sup>1</sup>

Received: 29 May 2021 / Revised: 7 October 2021 / Accepted: 13 October 2021 / Published online: 22 January 2022 © The Author(s), under exclusive licence to Springer-Verlag GmbH Germany, part of Springer Nature 2021

#### Abstract

Radio frequency electromagnetic noise (RF) of anthropogenic origin has been shown to disrupt magnetic orientation behavior in some animals. Two sources of natural RF might also have the potential to disturb magnetic orientation behavior under some conditions: solar RF and atmospheric RF. In this review, we outline the frequency ranges and electric/magnetic field magnitudes of RF that have been shown to disturb magnetoreceptive behavior in laboratory studies and compare these to the ranges of solar and atmospheric RF. Frequencies shown to be disruptive in laboratory studies range from 0.1 to 10 MHz, with magnetic magnitudes as low as 1 nT reported to have effects. Based on these values, it appears unlikely that solar RF alone routinely disrupts magnetic orientation. In contrast, atmospheric RF does sometimes exceed the levels known to disrupt magnetic orientation in laboratory studies. We provide a reference for when and where atmospheric RF can be expected to reach these levels, as well as a guide for quantifying RF measurements.

**Keywords** Solar storms · Lightning · Atmospheric radio frequency noise · Medium frequency and high frequency radio noise

#### Introduction

Although numerous animals detect Earth's magnetic field and use it as a cue in orientation and navigation, many aspects of this sensory modality remain enigmatic (Johnsen and Lohmann 2005; Rozhok 2008; Johnsen et al. 2020). One challenge in magnetoreception research is that magnetic orientation behavior can be highly variable. In certain cases, organisms that performed a task reliably at one time or in one location, behave differently at another time or in a new location (Rozhok 2008; Fleischmann et al. 2020; Johnsen et al. 2020). Although there are likely many reasons for these changes in behavior (Johnsen et al. 2020), a recent finding of interest is that radio frequency electromagnetic noise (RF) can, under certain circumstances, disrupt magnetic

orientation behavior (Ritz et al. 2004). This result has been demonstrated in a variety of organisms ranging from invertebrates to birds (e.g., Thalau et al. 2005; Vacha et al. 2009; Kavokin et al. 2014; Wiltschko et al. 2015; Schwarze et al. 2016; Tomanova and Vacha 2016; Pakhomov et al. 2017; Pinzon-Rodriguez and Muheim 2017). Thus, an intriguing possibility is that environmental sources of RF might contribute to behavioral inconsistencies in some magnetoreception studies (Begall et al. 2014; Engels et al. 2014; Malewski et al. 2018). Although much of the focus has been on anthropogenic RF, there are also several natural sources of RF that have the potential to disrupt magnetic orientation behavior. These natural RF sources pose important questions for the field of magnetoreception. For example, we have a limited understanding of when, and how often, these natural sources of RF reach levels high enough to disturb the orientation behavior of magnetoreceptive animals. If this occurs often, and over large regions of the earth, it might suggest that magnetic cues are not as reliable as previously thought, posing additional questions for magnetoreception research about how animals have learned to compensate for these disruptions.

There are two natural sources of RF that might, in principle, affect magnetoreceptive animals: solar activity and



<sup>☐</sup> Jesse Granger jngranger@email.wm.edu

Department of Biology, Duke University, Durham, NC, USA

Department of Electrical and Computer Engineering, Duke University, Durham, NC, USA

Department of Biology, University of North Carolina at Chapel Hill, Chapel Hill, NC, USA

atmospheric electrical storms. Both sources have extreme increases in RF emissions that can last for several hours. In addition, several correlative studies have shown a link between increased solar activity and disturbed magnetic navigation and orientation behavior (e.g., Yeagley 1951; Larkin and Keeton 1976; Klinowska 1986; Hart et al. 2013), which has been suggested to be mediated by solar RF (Winklhofer 2004; Kirschvink 2014; Granger et al. 2020). Although it is difficult to experimentally test whether these natural RF sources disturb magnetoreceptive animals, a first step is to determine if the magnitudes of these natural RF sources reach the levels shown to disturb animals in laboratory studies.

To assess the potential for these natural RF sources to disturb magnetoreception behavior, we perform a meta-analysis of previous behavioral experiments to identify general trends in the frequency ranges and magnitudes of RF known to disturb animals. We then outline the spatial and temporal distribution of both natural and anthropogenic sources of RF. Finally, we compare the values seen to disturb magnetoreceptive animals in the lab to the levels seen from natural sources of RF in order to better understand if, and how often, these RF sources might disturb magnetic orientation. Little work has been done in this area, largely because there are many ways to quantify an electromagnetic field, and it is not trivial to convert between them. We additionally provide a guide for quantifying RF, as well as formulas to convert between different RF measurements.

# Ranges of radio frequency noise shown to disrupt magnetic orientation behavior in laboratory studies

To test for RF disruption of magnetic orientation behavior, most studies first confirm that an animal reliably orients in a specific magnetic direction, and then show that this orientation is disrupted in the presence of RF. Because most experiments are conducted within the near-field region of their source (Box 1), using a magnetic-field-generating coil, there is often no measurable induced electric field in the testing arena—although electric fields generated from nearby equipment may still be present. For this reason, the stimuli used are more accurately referred to as an oscillating magnetic field rather than electromagnetic radiation. In keeping with conventions in the magnetoreception literature, however, we will refer to all stimuli used here as "RF," with the acknowledgement that this is a slightly misleading definition of the actual stimulus being measured. To identify the ranges of frequencies and magnetic/electric magnitudes of RF that affect orientation, we identified studies with comparable experimental set-ups, using the selection criteria described in the supplemental material.



#### **Box 1: electromagnetic fields**

Electromagnetic fields can contain both an electric and magnetic field. The magnitude of the electric field (E) is measured in volts per meter (V/m). The magnitude of the magnetic field is measured as the magnetic flux density (B) in Tesla (T). The regions around the source of an electromagnetic field can be roughly divided into the far-field and near-field, with the boundary between the two defined by the electromagnetic wavelength (Fig. 1).

Far-field: The far-field begins at a distance greater than one wavelength from the source; for 1–10 MHz RF, this would be a distance between ~ 30–300 m. The far-field contains propagating "radiative" waves, in which the electric and magnetic fields are orthogonal to both each other and the direction of propagation, and have magnitudes that exist in a fixed ratio (Fig. 1). In this region it is common to take a power flux measurement, reported in watts per meter squared (W/m²), because in the far-field it is simple to convert between power and the magnitudes of the magnetic and electric fields.

Near-field: The near-field encompasses distances within one wavelength of the source. In this region the magnetic and electric fields are decoupled and thus independent (Fig. 1). Because of this, it is important to measure both the electric and magnetic fields separately, as it is not possible to reliably convert from one to the other and a power flux measurement cannot adequately describe the conditions that exist. Within less than one half of a wavelength from the source, the type of field being produced by the specific source will generally dominate (i.e. a coil will produce a magnetic field without a measurable electric field), though electric fields generated by the device itself may still be present in the area, depending on the device geometry.

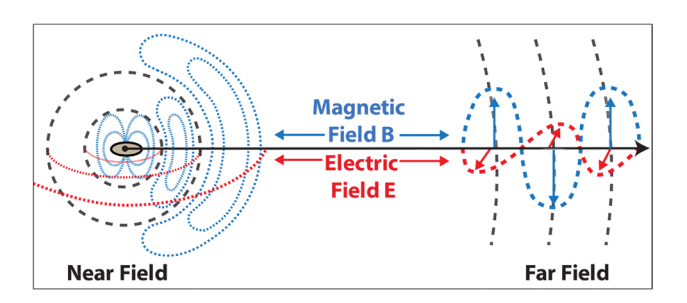


**Fig. 1** A symbolic representation of an electromagnetic field in the near and far-field. In the near-field there are spherical waves, and the electric and magnetic fields have no set relationship. In the far-field there are planar waves where the electric and magnetic fields are orthogonal, and their magnitudes are correlated. Adapted from (Marinissen et al. 2009)

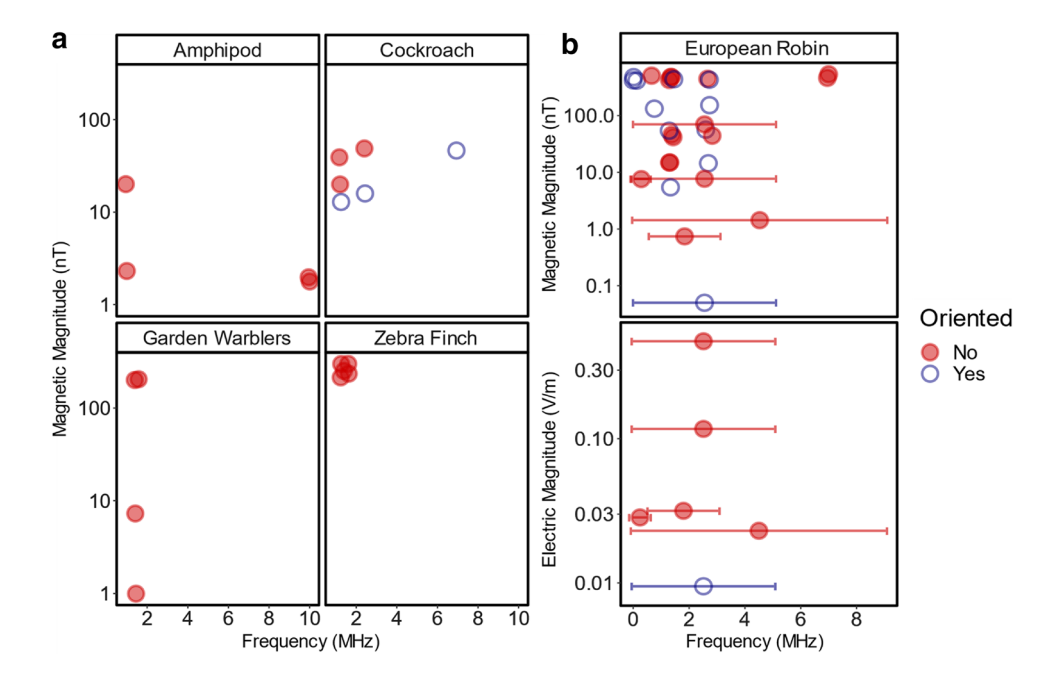


Fig. 2 The behavioral results reported with respect to the ranges of frequency and magnetic/electric magnitudes to which the animals were exposed. Unfilled, blue dots represent values at which animals oriented in the proper magnetic direction. Filled, red dots represent the values at which animals failed to orient in the proper magnetic direction. Behavioral results from narrowband RF lack a horizontal bar, while behavioral results from broadband RF have a centered hor-

izontal bar which indicates the total frequency range. For narrowband RF, the dots represent the amplitude of the magnetic field (Box 2), jittered for visualization. For broadband studies, the dots represent the  $B_{RMS}$  or  $E_{RMS}$  values, in average mode, of the magnetic and electric field respectively (Box 2). Data used to generate this figure can be found in the Tables S1 and S2, supplemental materials

Figure 2 summarizes studies of magnetic orientation behavior in the presence of RF, analyzed with regard to the electric and magnetic magnitudes and frequencies to which the animals were exposed. Importantly, there are many ways to quantify the magnitude of an electric or magnetic field, some of which yield different and noncomparable measurements. Detailed information about these methods is summarized in Appendix A, and the quantification methods used in this review are described in Box 2. Briefly, for narrowband RF (RF limited in frequency range), we report the amplitude of the magnetic field. For broadband RF (RF spanning a large frequency range,) we report the magnitude of both the electric and magnetic fields using a root-mean-squared (RMS) integration, abbreviated as B<sub>RMS</sub> for the magnetic field, and E<sub>RMS</sub> for the electric field. For narrowband studies, only the magnetic field was plotted because the electric field was almost never directly measured. Studies were not included if there was insufficient information to determine

### Box 2: measurements of narrowband vs broadband radio frequency noise

Electromagnetic field magnitudes can be measured and quantified in different ways, depending on whether the field is narrowband or broadband. A detailed discussion of these quantification methods can be found in Appendix A. Briefly:

Narrowband: Narrowband or single frequency RF spans a very small frequency range, (Fig. 3). The magnitude of narrowband RF can be measured as the amplitude of the sinusoidal, or nearly sinusoidal, wave. For example, in Fig. 3, the amplitude of the narrowband RF is ~50nT.

Broadband: Broadband RF spans a large frequency range (Fig. 3) and is measured by dividing the total frequency range into multiple frequency bins, and separate amplitude measurements are made for each bin. Thus, the measured magnitude will depend on the total frequency range, the size of the bins, or the resolution bandwidth (Appendix B), and the way the bins are integrated. In this review, we use a root mean squared (RMS) integration method for both the magnetic and electric fields, defined in Appendix A, and abbreviated here as  $B_{\text{RMS}}$  for the magnetic field and  $E_{\rm RMS}$  for the electric field. This method is independent of the resolution bandwidth of the detector (Appendix B) and, as a straight field amplitude, is most physically comparable to the amplitude measurement from narrowband RF (Kobylkov et al. 2019). The  $B_{\rm RMS}$  for the broadband signal in Fig. 3 is ~ 50 nT.



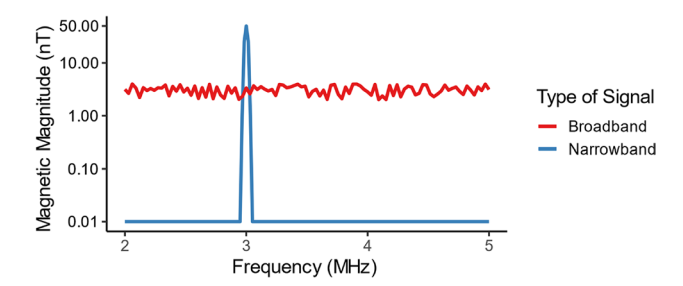


Fig. 3 An example of broadband (red) and narrowband (blue) RF

how the RF had been measured, such that it could be converted into other units. Finally, due to inevitable uncertainties in precisely how the data were processed by different studies, an error bar of at least  $\sqrt{2}$  should be assumed for all reported magnitude measurements, though it may be higher depending on device calibration (See Nießner and Winklhofer 2017 for recommendations on limiting error during measurement, and Kirschvink et al. 2010 for recommendations on device set up and controls). A summary table of all studies included can be found in the supplemental material (Tables S1 and S2).

Thus far, no study has shown that RF with a frequency less than 0.1 MHz disrupts magnetic orientation behavior, suggesting that this value may approximate the lower frequency bound for RF disruption (Fig. 2). Unfortunately, at this time, the upper frequency bound, and a lower electric or magnetic field magnitude bound at any frequency are unknown. Although some studies show that certain species are disrupted by far lower magnetic magnitudes near 1 MHz than at other frequencies (Ritz et al. 2009; Vacha et al. 2009), this is not seen across all experiments. For example, magnetic orientation of an amphipod (*Gondogeneia antarctica*) is disrupted at frequencies as high as 10 MHz with magnetic magnitudes as low as 20 nT, additionally suggesting that the effect may extend to higher frequencies than previously thought (Tomanova and Vacha 2016).

### The ionosphere, and sources of radio frequency noise

Although there is still much to learn, results indicate that RF within the frequency range of 1–10 MHz can, under at least some conditions, disrupt magnetic orientation. There are three sources of environmental RF in this same 1–10 MHz range that might, in principle, affect magnetoreceptive animals: anthropogenic, solar, and atmospheric (Desch 1990; Volland 1995). Figure 4 is a power spectral density plot (Box 3) of these sources of RF in comparison to the galactic background. The galactic background is a steady source of broadband electromagnetic radiation originating from the

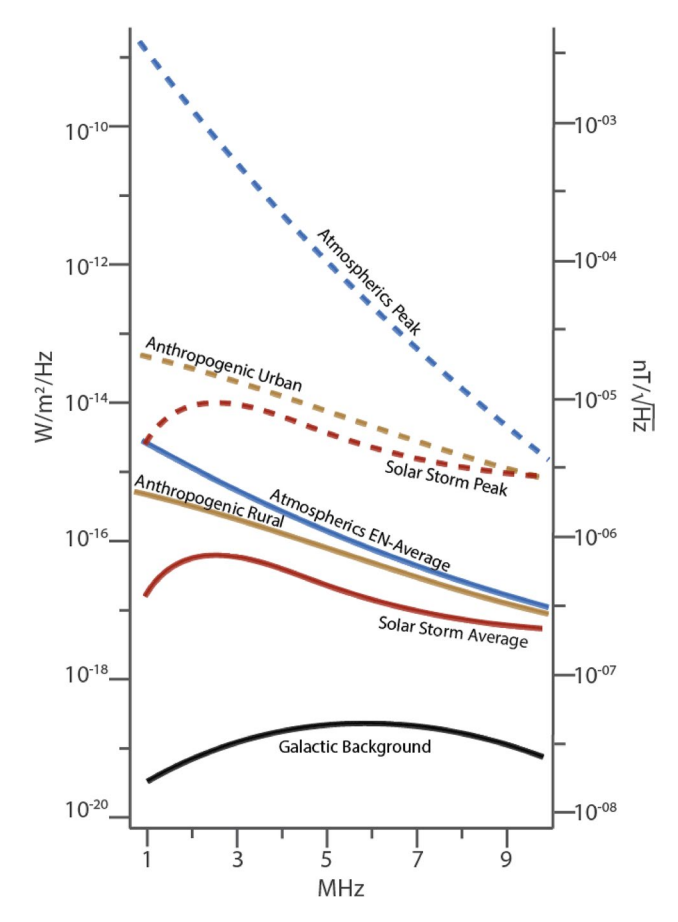


Fig. 4 Power spectral density of anthropogenic and natural RF, with the galactic background for comparison. Dotted lines are higher ranges; solid lines are lower ranges. The black line is the galactic background, gold lines are anthropogenic RF, red lines are solar radio storms, and blue lines are atmospheric RF. The "atmospherics EN-Average" is the average value seen near the equator (- 25 to 25 deg latitude), at night (16:00-4:00 Local Time). For anthropogenic RF and atmospherics, these are the values that would be measured on the surface of the earth. For the galactic background and solar storms these are the values that would be measured from a distance approximately half way to the moon and are not corrected for ionospheric shielding. Atmospheric data were digitized from (International Radio Consultive Committee 1983) (see supplemental material). Anthropogenic data were adapted from (International Telecommunication Union 2019), galactic background from (Zarka et al. 2012), and solar storm data from (Dulk 1990; Zarka et al. 2012). Note that these RF sources are not limited to this frequency range; additional information outside of these ranges are in the sources listed above

big bang and other extrasolar phenomena, and thus offers a reasonable lower bound for detectability.

In addition to the sources listed in Fig. 4, the earth's auroral kilometric radiation (AKR) is another powerful source of RF generated at night in polar regions (Desch 1990; Erickson 1990; Zarka et al. 2012). The AKR ranges from 50 to 700 kHz, peaking at approximately 200 kHz, though rare emissions at higher frequencies have been reported (Desch 1990). Notably, however, the AKR is generated at an altitude



#### Box 3: spectral density plots

Electromagnetic field measurements from multiple studies can be compared using spectral density plots. Spectra are used to show how the magnitude of the electric/magnetic fields varies over different frequencies; however, the measured magnitude depends on the resolution bandwidth of the receiving system (Appendix B). Thus, when comparing electromagnetic fields from multiple studies, it is helpful to use spectral density plots, in which the magnitude is normalized to a one Hertz resolution bandwidth. This can be done by dividing the magnitude by the square root of the receiver's resolution bandwidth in Hertz. When measurements are taken in the near-field region, electric spectral densities and magnetic spectral densities should be plotted separately, but when measurements are taken in the far-field region, plotting the power spectral density is sufficient.

of approximately 3,000–20,000 km, well above the ionosphere, and thus is predominantly reflected towards space, and does not make it to the earth's surface (Desch 1990; Lamy et al. 2010). Because of this, it seems unlikely that the

AKR would have any relevant biological impact and is not covered in this review.

In this section, we explore the origins, ranges, and temporal aspects of the anthropogenic and natural sources of RF outlined in Fig. 4. To understand how these environmental sources of RF vary, however, we must first discuss the ionosphere, and its impact on the ways electromagnetic radiation is propagated across the earth.

#### The ionosphere

The ionosphere is the outer-most layer of Earth's atmosphere and extends from approximately 50 km to 1,000 km above the earth's surface. It is composed of several layers, but the D-layer and the F-layer are the most important for radio-wave propagation and transmission (Fig. 5). On the day side of the earth, both the D-layer and F-layer are present, while on the night-side of the earth, only the F-layer is present. Radio frequency waves in the kHz range are absorbed by the D-layer or reflected off the F-layer when the D-layer is not present (Davies 1965; Al'pert 1973; Poole 2003). At higher frequencies, radio frequency waves are able to pass through the D-layer, when it is present, and are also reflected off

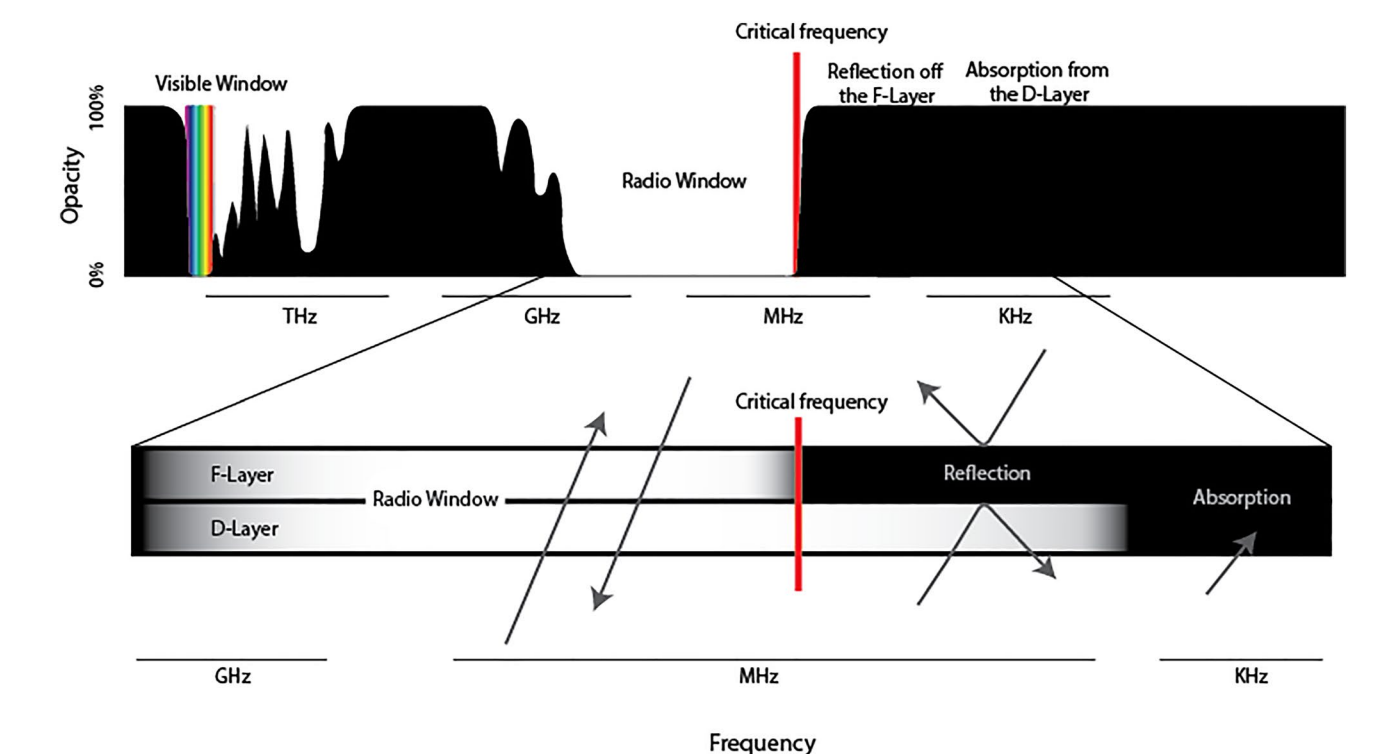


**Fig. 5** Electromagnetic (EM) radiation propagation through the atmosphere. The atmosphere is opaque to most frequencies except for the visual window and the radio window. The radio window extends from approximately 30 GHz to the critical frequency, which ranges from ~1–30 MHz. In the MHz range, EM waves at frequencies higher than the critical frequency pass through the ionosphere, whereas EM

waves at frequencies lower than the critical frequency are reflected off the F-layer. EM waves in the kHz range are absorbed by the D-layer when it is present. Note that during the night, when the D-layer is not present, these frequencies are reflected off the E- and F-layers (Poole 2003). Absorption spectra image credit: NASA (public domain)



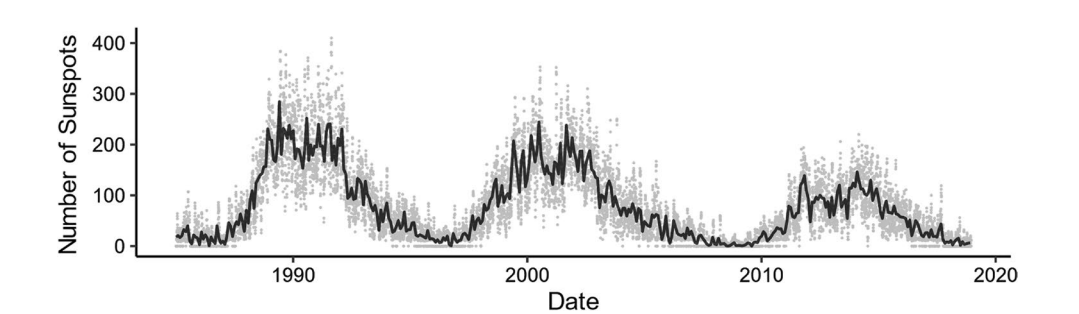
#### Box 4: solar weather

The solar cycle: The solar cycle is an 11-year periodicity in the overall activity of the sun. It can be monitored by counting the number of sunspots, which are relatively dark areas of increased magnetic flux on the surface of the sun (Fig. 6). Solar storms generally originate from these darkened areas. Thus the number of sunspots is tightly correlated to the overall level of solar activity (Davies 1965; Cander 2019).

**Solar storms:** A solar storm consists of a sudden and extreme increase in the electromagnetic radiation and/ or particle emissions from a region on the sun. These storms can last anywhere from a few minutes to several days and have the capacity to significantly disturb Earth's magnetic field and ionosphere. A detailed discussion of the different categories of storms can be found in (Cander 2019). Every storm is unique, and the characteristics of any individual storm will differ in magnitude across the electromagnetic spectrum and in particle composition (Davies 1965; Kavokin et al. 2014; Pakhomov et al. 2017; Cander 2019). Storms accompanied by a large increase in radio-frequency electromagnetic noise are referred to as solar radio storms. Radio storms can range in frequency from 10 kHz to 1 GHz and last for days in extreme cases (Davies 1965; Dulk 1990; Krupar et al. 2014; Pinzon-Rodriguez and Muheim 2017).

the F-layer. The maximum horizontal distance a radio-wave reflected off the F-layer might travel across the surface of the earth is around 4,000 km (Poole 2003). As the frequency of a radio wave is increased, it will reach what is referred to as the "critical frequency," at which point it passes through the F-layer. The range of radio frequencies that pass through all the layers of the ionosphere is referred to as the "radio window," which lies between the critical frequency and approximately ~ 30 GHz, at which point waves are absorbed by atmospheric gases, such as CO<sub>2</sub>, and water vapor (Fig. 5) (Davies 1965; Al'pert 1973; Poole 2003).

Fig. 6 The solar cycle from 1980–2018 as measured by the number of sunspots. Gray dots are the daily number of sunspots, and the black line is the monthly mean. Sunspot data from the World Data Center SILSO, Royal Observatory of Belgium, Brusselss (SILO World Data Center 2021)





The critical frequency is not stable and can range anywhere from 1-30 MHz depending on when and where it is measured. Thus, the value of the critical frequency has important implications for 1-10 MHz RF propagation and transmission. For example, any extra-terrestrial RF below the critical frequency will not be able to penetrate the ionosphere and reach the surface of the earth. Similarly, earth-based RF sources that exceed the critical frequency will escape the ionosphere into space, while RF at frequencies below the critical frequency will be reflected off the F-layer and sometimes propagate over thousands of kilometers across the earth's surface (Fig. 5) (Poole 2003). The critical frequency can be approximated using a measurement called the foF2 and is affected by several different factors (Davies 1965; Al'pert 1973; Poole 2003; Cander 2019). Among these are: location—the critical frequency is typically lower near the poles than the equator (Davies 1965); time of day—the critical frequency is lower during the night than the day (Davies 1965; Desch 1990); the solar cycle—the critical frequency is lower during the solar minimum than the solar maximum (Box 4) (Davies 1965; Erickson 1990; Cander 2019); and solar storms (Box 4). Of the various factors that alter the critical frequency, the effect of a solar storm is particularly difficult to predict. It depends, in a complicated fashion, on the location, time of day, season, and stage of the storm. Storms can either increase the critical frequency, decrease it, or have both effects at different stages of the same storm (Davies 1965; Blagoveshchensky 2014; Shubin and Deminov 2019).

#### Anthropogenic radio frequency noise

RF in the 1–10 MHz range is generated by many electronic devices, including televisions, cell phones, car ignitions, electric heaters, and AM radios (Bianchi and Meloni 2007). The magnitude of RF generated by these devices varies greatly and decreases with distance from the source. The average radiative power of RF in urban and rural areas is shown in Fig. 4, although it should be noted that sources of anthropogenic RF are sometimes close enough to be in the near-field region (Box 1). When this is the case, converting from the power spectral density to the magnetic/electric fields can result in measurements several orders of magnitude different from what actually exists in the area.

Evidence suggests anthropogenic levels of RF are sufficient to disturb magnetic orientation behavior under some conditions. For example, several researchers have noted that, when in an urban area, it is necessary to shield their experimental apparatus from RF in order for animals to orient with a magnetic field (Phillips et al. 2013; Begall et al. 2014; Malewski et al. 2018). In addition, it has been observed that spontaneous magnetic orientation behavior in certain ruminants is disturbed near power lines (reviewed in Begall et al. 2014), though power lines generally only produce RF at or near 50-60 Hz, and higher frequency noise generation is rare, often occurring because of faulty equipment (Pakala and Chartier 1971). Engles et. al. conducted a series of experiments to test whether the anthropogenic levels of RF on campus at the University of Oldenburg were sufficient to disturb the magnetic orientation behavior of European robins. Results revealed that, when the experimental arena was shielded from RF on campus the birds oriented magnetically but failed to do so when the shielding was removed. In contrast, the birds oriented magnetically without shielding in a rural area (Engels et al. 2014).

#### Solar radio frequency noise

Increases in electromagnetic radiation and energetic particle emissions from the sun are caused by disturbances in the sun's corona. Both slow and fast changes to the sun's emissions, referred to as "solar weather," can disturb the earth's magnetosphere and ionosphere (Box 4) (Davies 1965; Cander 2019). Indeed, several studies have suggested that animal's magnetic orientation behavior might, in some cases, vary over the solar cycle or during a solar storm (e.g., Kowalski et al. 1988; Vanselow and Ricklefs 2005; Schiffner and Wiltschko 2011; Fitak et al. 2020), with a decrease in animals' navigational or orientation abilities occurring on days with increased solar activity. The strength of this effect seems to vary depending on location (Keeton et al. 1974). It has been hypothesized that this correlation may be mediated by solar RF (Winklhofer 2004; Kirschvink 2014; Granger et al. 2020).

The number of solar radio storms per year varies greatly over the course of the 11-year solar cycle, with almost no solar radio storms measured during the solar minimum (Box 4) (Kaiser 2003; Krupar et al. 2014). Average and peak power spectral density measurements of solar radio storms in the 1–10 MHz range are shown in Fig. 4; it is important to note; however, that these measurements do not account for ionospheric shielding, and the values seen on the surface of the earth depend greatly on the critical frequency. A spectral density plot of a solar radio storm that was recorded by both a terrestrial and space-based telescope, and thus demonstrates the effect of ionospheric shielding, is shown in Fig. 7 (Dulk et al. 2001).

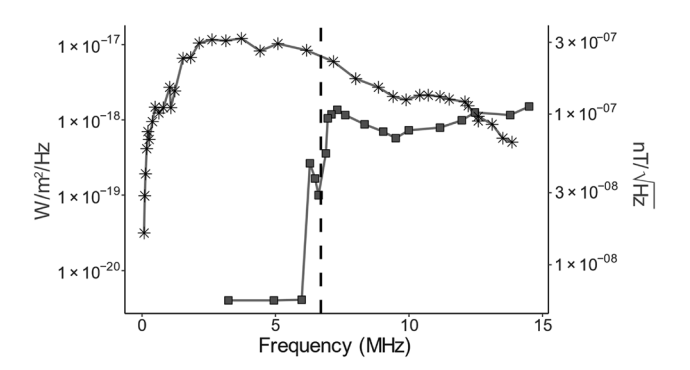


**Fig. 7** Spectral density plot of a solar radio burst that occurred around 0120 UT on 3 January 1998. The stars and squares mark the spectra observed by the space-based observatory, WAVES and the terrestrial radio telescope, BIRS respectively. The vertical dotted line at 6.7 MHz represents the foF2 at that time near the BIRS observatory in Hobart, Tasmania, Australia, as obtained from the Australian Bureau of Meteorology's World Data Centre archives for hourly ionospheric data. Figure adapted from (Dulk et al. 2001)

#### **Atmospherics**

In addition to solar RF, the only other dynamic source of natural RF in the 1-10 MHz range is a phenomenon referred to as atmospherics. Although this category includes RF generated by atmospheric gases and water vapor, most atmospheric RF is due to lightning (Coleman 2002; Pan and Li 2014; Pederick and Cervera 2016). RF due to lightning can be separated into two components: local and propagated. The high-magnitude local RF is due to nearby thunderstorms and consists of short bursts within the roughly one-second duration of a lightning flash. In contrast, the lower-magnitude propagated RF is due to the contribution of many thunderstorms occurring far away, with the RF then being reflected by the ionosphere and traveling long distances (Coleman 2002; Pan and Li 2014; Pederick and Cervera 2016). This propagated component can be measured as nearly continuous low-level background RF (Coleman 2002; Pan and Li 2014; Pederick and Cervera 2016). Across the earth there are as many as 100 lightning strikes occurring per second; however, the distribution of thunderstorms is highly uneven across time and space (Coleman 2002; Pan and Li 2014; Pederick and Cervera 2016). Both thunderstorm activity and ionospheric conditions affect the average levels of propagated atmospheric RF that occur in an area at any time.

Levels of atmospheric RF are generally highest near the equator, with peak values predominantly found between – 25° and 25° latitude. Elevated levels also occur at higher latitudes but are generally limited to the North American region and occur primarily in the spring and summer. In addition, atmospheric RF levels are almost always higher at night than during the day due to the absence of the absorptive D-layer of the ionosphere and an increase in



thunderstorm activity (Kotaki 1984; Coleman 2002; Pan and Li 2014; Pederick and Cervera 2016). The power spectral density of peak atmospheric RF, as well as the average levels seen near the equator at night, are shown in Fig. 4.

### Comparing environmental sources of radio frequency noise to laboratory thresholds

Although anthropogenic RF has been shown to disrupt magnetic orientation behavior in some cases, no comparisons have been made between the magnitude of the electric and magnetic fields of natural sources of RF and the ranges known to disturb orientation in laboratory studies. Analyses suggest that peak atmospheric RF, and the average levels of atmospheric RF seen near the equator at night, fall well within or above levels shown to disturb several species of animals in both broadband and narrowband studies (Fig. 8a). In contrast, peak solar RF falls below the values shown to disturb magnetic orientation in any animal thus far (Fig. 8a).

We additionally compared the magnetic and electric spectral densities (Box 3) of these natural sources of RF to the range in which we expect the lower laboratory threshold may lie for broadband RF (Fig. 8b). These spectral density plots preserve frequency-dependent information and can provide

further information about these sources. For example, it is apparent from these spectral density plots that atmospheric RF is greatest at lower frequencies. In fact, for the average levels near the equator at night, the only frequencies that fall into the range for the lower laboratory threshold are below 1 MHz. For atmospheric RF, these lower frequencies are the least likely to be impacted by shifts in the critical frequency but are the most likely to be affected by the absorptive D-layer of the ionosphere.

Finally, we estimated where and when levels of atmospheric RF exist that have the potential to disturb magnetic orientation behavior. From Fig. 8b, we show that the laboratory threshold for the magnetic magnitude at 1 MHz likely lies above approximately  $5 * 10^{-5} \text{nT} / \sqrt{\text{Hz}}$ . The International Radio Consultative Committee (CCIR) made global, long-term measurements of average atmospheric RF levels over four-hour time periods, across all four seasons (International Radio Consultive Committee 1983). In Fig. 9, we summarize the geographical and temporal trends from the CCIR for average levels of atmospheric RF that were above  $5 * 10^{-5}$ nT/ $\sqrt{\text{Hz}}$  at 1 MHz. In general, propagated atmospheric RF at levels that are sufficient to disturb a magnetoreceptive animal occur frequently between the hours of 16:00–4:00 (local time), in the tropics across all seasons, and over central North America in the spring and summer.

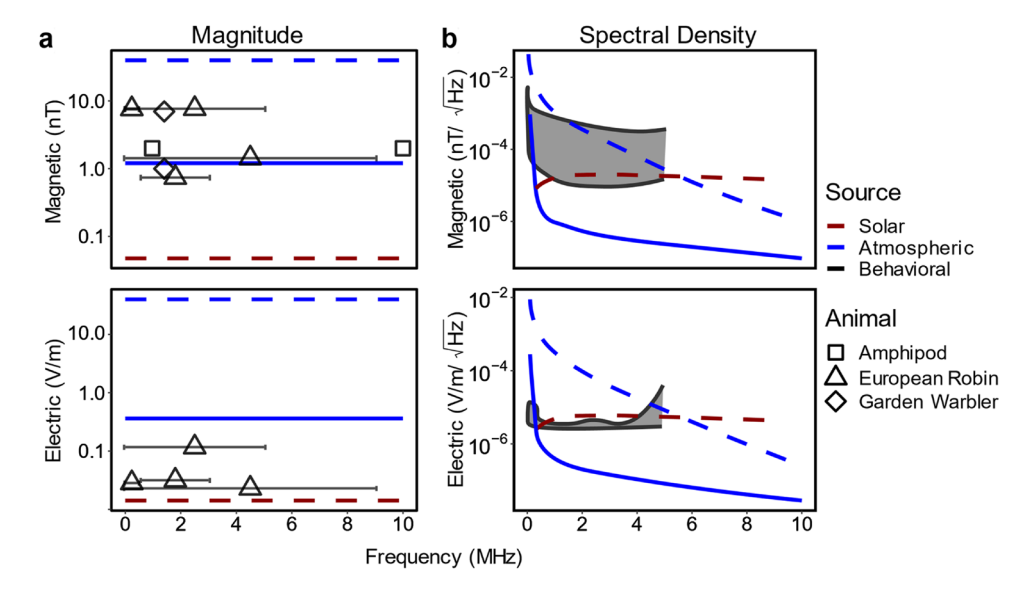
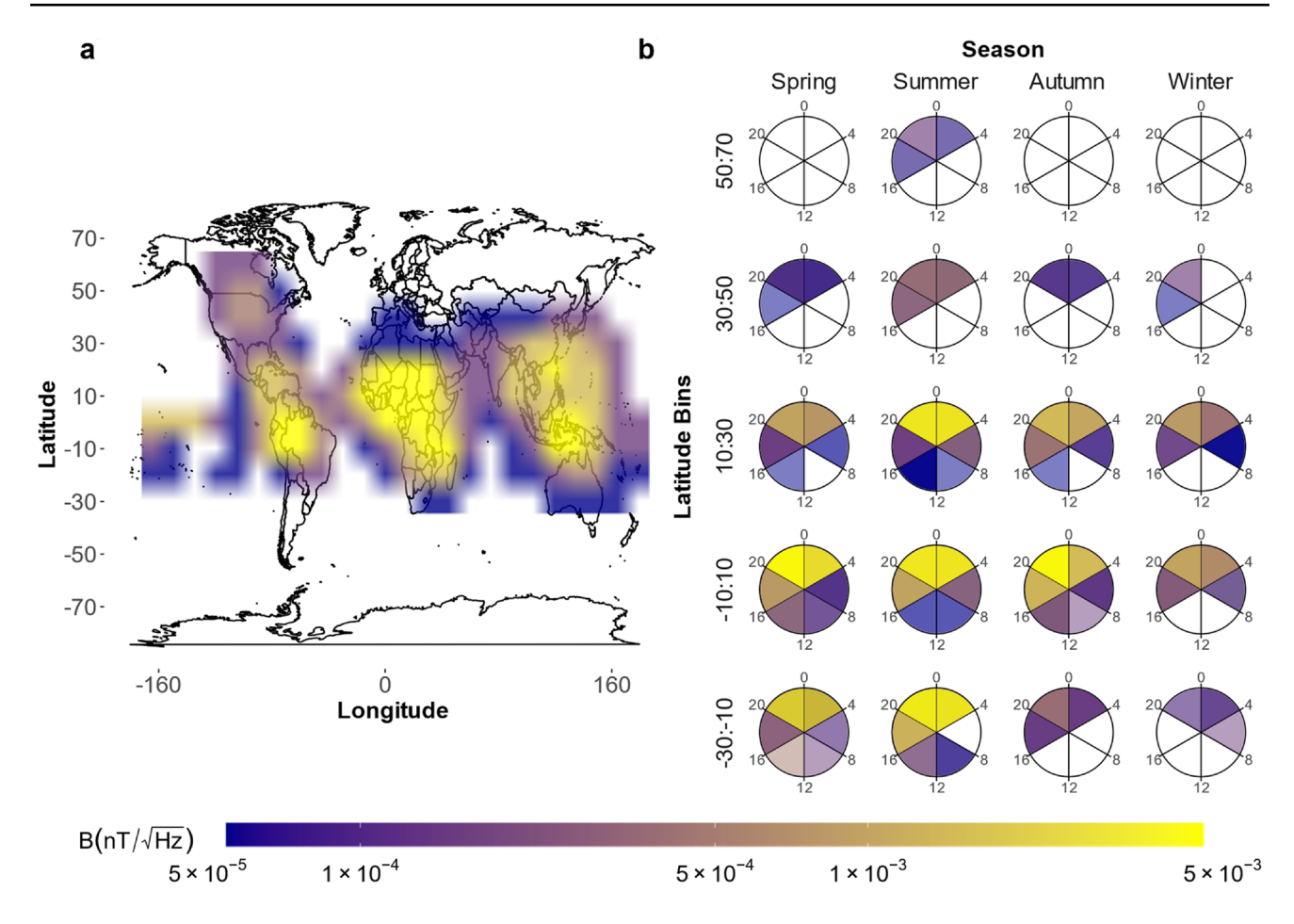


Fig. 8 a Levels of RF known to disrupt magnetic orientation in laboratory studies compared to atmospheric and solar RF. Black points with no bars correspond to the four lowest magnetic magnitudes reported to disturb orientation in narrowband studies. The black points with bars correspond to the four lowest  $B_{RMS}$  and  $E_{RMS}$  levels reported to disrupt orientation in broadband studies, where the horizontal bars indicate the total frequency range. The shapes of the black points correspond to the animals tested. These are compared to the  $B_{RMS}$  and  $E_{RMS}$  levels for peak atmospheric (blue, dotted), peak solar (red, dotted), and the EN-average atmospheric RF (blue, solid), integrated from 0.1–10 MHz. b Electric and magnetic spectral densi-

ties of the peak atmospheric (blue, dotted), peak solar RF (red, dotted), and EN-average atmospheric (blue, solid) levels of RF. The gray shaded area is the range within which the lower laboratory threshold for disturbance may lie. The upper gray line is the lowest broadband RF an animal has been disturbed by, and the lower gray line is the highest broadband RF no animal has been disturbed by. Formulas used to convert these natural sources of RF from power-spectral density to the magnetic and electric fields are in supplemental material. Solar RF is the value as would be measured from a distance approximately halfway to the moon and is not corrected for ionospheric shielding





**Fig. 9** Spatial and temporal distribution of the propagated levels of Atmospheric RF above  $5*10^{-5}$  nT/ $\sqrt{\text{Hz}}$  at 1 MHz. Figure a shows the spatial distribution, with most hot spots occurring between -25 to 25 deg latitude, or over central North America. Figure b shows the temporal distribution. The central clocks mark the time of day

at which elevated levels are seen, in 4-h periods (LT). The columns represent the season, and the rows represent the latitudinal ranges at which these values are seen. The color bar shows the magnetic magnitude of the RF. Data digitized from the CCIR report 322–2 (International Radio Consultive Committee 1983)

It is important to note that the magnitude measurements from these natural sources of RF are far more time varying than the RF used in laboratory studies. The magnitude measurements from atmospherics and solar RF are the mean values taken in highly variable environments, and thus their impact on animal behavior may be different than what is seen under the steady RF used in laboratory experiments. Thus far, no experiment has tested the effect of highly time-varying RF on magnetoreceptive behavior, though it has been shown that rodents exposed to an "RF sweep," in which the frequency was varied between 0.9 and 5 MHz in one msec intervals, changed the magnetic direction in which they preferred to build their nests (Malkemper et al. 2015).

### **Conclusions and suggestions for future research**

Although it is evident that RF has a deleterious effect on magnetic orientation in some species, the exact ranges of frequencies and magnetic field magnitudes responsible for this effect remain to be determined. Frequencies seen to be disruptive range from 0.1 to 10 MHz, and disruptive magnetic magnitudes are found as low as 1 nT. Future research should attempt to determine an upper frequency bound, as well as lower electric and magnetic magnitude bounds at different frequencies.



Given the laboratory thresholds seen thus far, it appears unlikely that solar RF alone routinely disrupts magnetic orientation. Still, it is possible that other effects of solar storms, such as disruptions to the earth's magnetosphere, might impact geomagnetic navigation under some conditions. In addition, it is possible that the correlations seen between general solar activity and disturbed magnetic orientation might be due to changes in ionospheric propagation of RF. In other words, because the critical frequency is strongly linked to the solar cycle, navigational disturbances might be in turn linked to increased propagation of atmospheric or anthropogenic RF (Kotaki 1984; Ward and Golley 1991).

Atmospheric RF can exceed the levels known to disrupt magnetic orientation in laboratory studies. Hot spots for atmospheric RF are typically seen between the hours of 16:00-4:00 (local time), near the equator across all seasons, and over North America in the spring and summer. These atmospheric RF hotspots may provide an additional explanation for why magnetoreceptive animals do not seem to rely exclusively on this sensory modality (Johnsen et al. 2020); indeed, there may be areas of the globe where the sense is largely unreliable. In addition, atmospheric RF may provide an explanation for variation in behavioral results, and researchers in these known hot spots should monitor the ambient levels of RF during their experiments. Importantly, atmospheric RF is highly time-varying in magnitude and may affect animals differently than the continuous and steady RF generated in lab. Future research on the impact of atmospheric RF on magnetoreceptive behavior may enhance understanding of the landscape in which this sense evolved.

#### **Appendix A**

In this appendix we explain the procedures typically used to quantify RF, provide guidance for converting between these methods, and summarize the methods used in this paper. As described below, electromagnetic fields are measured and quantified in different ways depending on whether they are narrowband or broadband.

'Narrowband,' or 'single frequency' RF spans a very small frequency range (Box 2). For narrowband RF, the magnitude of the electric or magnetic field is measured as either: (1) peak amplitude, or (2) Root-Mean-Square (RMS) amplitude. The relationship between an RMS amplitude and a peak amplitude depends on the waveform of the RF. For example, for a sinewave, peak amplitude =  $\sqrt{2}$ \*RMS amplitude. While the relationship between peak and RMS amplitudes is known for all continuous, periodic waveforms, there is no such relationship for an arbitrary nonperiodic waveform. Because of this, most signal analyzers will report an RMS amplitude. For all data plotted in this review, RMS amplitude was used; however, often narrowband

measurements are referred to simply as the "amplitude" or the "intensity" and no further information is given. In this case, we assumed the measurement was an RMS amplitude.

'Broadband' RF contains energy at many frequencies and often a continuum of frequencies (Box 2). Broadband RF is measured by dividing the overall frequency range into multiple frequency bins, and separate amplitude measurements are made for each bin. The amplitude measured within each bin will thus depend on the bin-size, or the resolution bandwidth of the measurement system (see Appendix B). In addition, the amplitude measured within each bin must then be integrated across time. Finally, to report a single magnitude measurement for broadband RF, one must integrate across the total frequency range. There are several ways to perform both of these integrations, many of which are noncomparable and can yield extremely different results. Because the magnetoreceptor is yet unknown, there is no way to determine which methods are most appropriate for quantifying how a magnetoreceptive animal perceives RF. Thus, it is imperative that any broadband study report their resolution bandwidth, methods of integration and provide a plot of the measured amplitude spectrum across frequencies. Without these details, it is not possible to convert between these different measurement methods. Here we summarize a few common integration methods across time and frequency for broadband RF:

Time: Broadband measurements cannot be taken instantaneously, and the amplitude at any one frequency will vary as the measurement is being taken. Most instruments integrate over time using either 'average' mode or 'max-hold' mode. The average mode computes the mean amplitude seen within each bin during the measurement duration, and the max-hold mode reports the maximum amplitude recorded within each bin at any point in time during the measurement duration. For white noise, and a sufficiently long measurement duration, average=  $\sqrt{10}$  \* max-hold (Kobylkov et al. 2019). All data plotted in this review were either made in average mode or converted to average mode using the conversion for white noise.

<u>Frequency:</u> Different researchers have used many different methods to integrate across their total frequency range, as summarized in (Kobylkov et al. 2019). For several reasons we recommend

$$B_{\rm RMS} = \sqrt{\Delta f} \sqrt{\frac{1}{N} \sum_{i=1}^{N} b_i^2} \tag{1}$$

where,  $\Delta f$  =total frequency range, N= number of bins integrated across,  $B_i$  =the amplitude of each individual frequency bin, RBW = resolution bandwidth and  $b_i = \frac{B_i}{\sqrt{\text{RBW}}}$  (Kobylkov et al. 2019). First, because it uses  $b_i$  instead of  $B_i$  it is not dependent on the resolution of the receiver (Appendix B). In other words, another measurement



taken with a different resolution bandwidth will still yield the same result. In addition,  $B_{RMS}$  is proportional to the square root of the power density and is the most comparable to the narrowband amplitude measurements. There are situations where other frequency-integration methods may be more appropriate, as discussed in (Kobylkov et al. 2019); however, it is not always possible to convert these integration methods directly. Thus, raw spectra should be included for all broadband measurements, along with the resolution bandwidths used, so that they can be re-integrated using a different method when required. For all broadband data plotted in this review, raw spectra were digitized from the original paper and converted into  $b_i$  by dividing by the square root of the receiver resolution bandwidth and integrated using formula 1 above.

#### **Appendix B**

In this review, resolution bandwidth refers to the resolution of a measuring system, i.e., how finely the measuring device divides up the total frequency space of broadband RF before measuring the amplitude within each bin (Appendix A). In some papers, the term 'bandwidth' is used to refer to the total frequency range; however, the convention used in magnetoreception studies is to use 'bandwidth' to refer to the resolution of the measuring device. To avoid confusion, we thus use the term 'resolution bandwidth.' In this appendix, we report the ways in which to account for the resolution of a system for both broadband and narrowband RF (Box 2).

For broadband RF, this resolution has a significant impact on the amplitude reported by the measurement system. There are thus two options to fully specify the nature of the field. One is to provide a plot of the measured amplitude spectrum and also clearly specify the measurement resolution. If the measurement frequency resolution is not provided, then one cannot distinguish higher fields measured with a narrow frequency resolution from lower fields measured with a wide frequency resolution. The second option is to report the measured amplitude spectrum divided by the square root of the measurement resolution in Hz. This measurement is typically called a spectral density (Box 3) and yields a quantity that is independent of the measurement resolution.

For narrowband RF, the amplitude reported by the measurement system does not depend on the measurement resolution because increasing the measurement resolution bandwidth will not allow more energy into the measurement system. In this case, the first option of simply reporting the amplitude without the resolution bandwidth normalization is common. However, to eliminate any ambiguity, it is generally the best to report the resolution bandwidth and provide a spectrum for all RF types.

**Supplementary Information** The online version contains supplementary material available at https://doi.org/10.1007/s00359-021-01516-z.

**Acknowledgements** We thank the reviewers, as well as Alex Davis, Sarah Solie, Ryan Wilmington, and Drs. Eleanor Caves, Robert Fitak, for comments on the manuscript, and Drs. Jason Kooi, Henrik Mouritsen and Kassim Namir, for assistance in data interpretation.

**Author contributions** JG and SJ conceived the work; JG performed the literature search, compiled the data, and wrote the manuscript; SAC provided advice and information on electrical engineering and physics background; All authors were involved in the discussion of the results and critical revision of the manuscript.

**Funding** S.J. and K.J.L. were supported in part by a grant from the Air Force Office of Scientific Research [FA9550-20–1-0399]. J.G. was supported by a National Defense Science & Engineering Graduate Fellowship. S.A.C. was supported by the National Science Foundation [2026304].

Data availability All data used is provided in the supplemental.

#### **Declarations**

**Conflict of interest** The authors have no conflicts of interest to declare that are relevant to the content of this article.

#### References

Al'pert IAL (1973) Radio wave propagation and the ionosphere. Consultants Bureau, New York

Begall S, Burda H, Malkemper EP (2014) Chapter two—magnetore-ception in mammals. In: Naguib M, Barrett L, Brockmann HJ et al. (eds) Advances in the study of behavior, vol 46. Academic Press, pp 45–88. https://doi.org/10.1016/B978-0-12-800286-5.00002-X

Bianchi C, Meloni A (2007) Natural and man-made terrestrial electromagnetic noise: an outlook. Ann Geophys 50(3):435–445. https://doi.org/10.4401/ag-4425

Blagoveshchensky DV (2014) Variations in the critical frequency of the ionospheric F-region during magnetic storms in 2008–2012 at auroral latitudes. Geomag Aeron 54(5):568–574. https://doi.org/10.1134/S0016793214050028

Cander L (2019) Ionospheric space weather. Springer International Publishing, Cham. https://doi.org/10.1007/978-3-319-99331-7\_3

Coleman CJ (2002) A direction-sensitive model of atmospheric noise and its application to the analysis of High-Frequency receiving antennas. Radio Sci 37(3):3-3–10. https://doi.org/10.1029/2000R S002567

Davies K (1965) Ionospheric Radio Propagation. U.S. Dept. of the Commerce, National Bureau of Standards, Washington, D.C.

Desch MD (1990) A quantitative assessment of radio frequency interference in the near-earth environment. In: Lecture notes in physics, 1990. Low frequency astrophysics from space. Springer, Berlin, Heidelberg, pp 70–78. https://doi.org/10.1007/3-540-52891-1\_109

Dulk GA (2021) Solar radio astronomy at low frequencies. In: Berlin, Heidelberg, 1990. Low Frequency Astrophysics from Space. Springer, Berlin Heidelberg, pp 83–96

Dulk GA, Erickson WC, Manning R, Bougeret J-L (2001) Calibration of low-frequency radio telescopes using the galactic background



- radiation. Astron Astrophys 365(2):294–300. https://doi.org/10.1051/0004-6361:20000006
- Engels S, Schneider NL, Lefeldt N, Hein CM, Zapka M, Michalik A, Elbers D, Kittel A, Hore PJ, Mouritsen H (2014) Anthropogenic electromagnetic noise disrupts magnetic compass orientation in a migratory bird. Nature 509(7500):353–356. https://doi.org/10.1038/nature13290
- Erickson WC (1990) Radio noise near the earth in the 1–30 MHz frequency range. In: Kassim NE, Weiler KW (eds) Space. Lecture notes in physics, 1990. Low frequency astrophysics from space. Springer, Berlin Heidelberg, pp 57–69. https://doi.org/10.1007/3-540-52891-1 108
- Fitak RR, Wheeler BR, Johnsen S (2020) Effect of a magnetic pulse on orientation behavior in rainbow trout (*Oncorhynchus mykiss*). Behav Processes 172:104058. https://doi.org/10.1016/j.beproc. 2020 104058
- Fleischmann PN, Grob R, Rossler W (2020) Magnetoreception in Hymenoptera: importance for navigation. Anim Cogn. https://doi.org/10.1007/s10071-020-01431-x
- Granger J, Walkowicz L, Fitak R, Johnsen S (2020) Gray whales strand more often on days with increased levels of atmospheric radio-frequency noise. Curr Biol 30(4):R155–R156. https://doi.org/10.1016/j.cub.2020.01.028
- Hart V, Nováková P, Malkemper EP, Begall S, Hanzal V, Ježek M, Kušta T, Němcová V, Adámková J, Benediktová K, Červený J, Burda H (2013) Dogs are sensitive to small variations in the Earths magnetic field. Front Zool 10:80. https://doi.org/10.1186/ 1742-9994-10-80
- International Radio Consultive Committee (1983) Characteristics and applications of atmospheric radio noise data. Technical Report. Geneva
- International Telecommunication Union (2019) Recommendation ITU-R P.372–14. Technical Report. P Series. Radiowave propagation. ITU, Geneva
- Johnsen S, Lohmann KJ (2005) The physics and neurobiology of magnetoreception. Nat Rev Neurosci 6(9):703–712. https://doi.org/10.1038/nrn1745
- Johnsen S, Lohmann KJ, Warrant EJ (2020) Animal navigation: a noisy magnetic sense? J Exp Biol. https://doi.org/10.1242/jeb.164921
- Kaiser ML (2003) Solar radio emissions at solar maximum: Interplanetary perspective. Adv Space Res 32(4):461–465. https://doi.org/10.1016/S0273-1177(03)00330-2
- Kavokin K, Chernetsov N, Pakhomov A, Bojarinova J, Kobylkov D, Namozov B (2014) Magnetic orientation of garden warblers (*Sylvia borin*) under 14 MHz radiofrequency magnetic field. J R Soc Interface 11(97):20140451. https://doi.org/10.1098/rsif.2014.0451
- Keeton W, Larkin T, Windsor D (1974) Normal fluctuations in the earth's magnetic field influence pigeon orientation. J Comp Physiol A 95:95–103. https://doi.org/10.1007/BF00610108
- Kirschvink JL (2014) Radio waves zap the biomagnetic compass. Nature 509(7500):296–297. https://doi.org/10.1038/nature13334
- Kirschvink JL, Winklhofer M, Walker MM (2010) Biophysics of magnetic orientation: strengthening the interface between theory and experimental design. J R Soc Interface 7(suppl\_2):S179–S191. https://doi.org/10.1098/rsif.2009.0491.focus
- Klinowska M (1986) Cetacean live stranding dates relate to geomagnetic disturbances. Aquat Mamm 11(3):109–119
- Kobylkov D, Wynn J, Winklhofer M, Chetverikova R, Xu J, Hiscock H, Hore PJ, Mouritsen H (2019) Electromagnetic 0.1–100 kHz noise does not disrupt orientation in a night-migrating songbird implying a spin coherence lifetime of less than 10 micros. J R Soc Interface 16(161):20190716. https://doi.org/10.1098/rsif.2019.0716
- Kotaki M (1984) Global distribution of atmospheric radio noise derived from thunderstorm activity. J Atmos Terr Phys 46(10):867–877. https://doi.org/10.1016/0021-9169(84)90026-6

- Kowalski U, Wiltschko R, Fuller E (1988) Normal fluctuations of the geomagnetic field may affect initial orientation in pigeons. J Comp Physiol A 163:593–600. https://doi.org/10.1007/BF00603843
- Krupar V, Maksimovic M, Santolik O, Kontar EP, Cecconi B, Hoang S, Kruparova O, Soucek J, Reid H, Zaslavsky A (2014) Statistical survey of type III radio bursts at long wavelengths observed by the solar TErrestrial RElations observatory (STEREO)/waves instruments: radio flux density variations with frequency. Sol Phys 289(8):3121–3135. https://doi.org/10.1007/s11207-014-0522-x
- Lamy L, Zarka P, Cecconi B, Prangé R (2010) Auroral kilometric radiation diurnal, semidiurnal, and shorter-term modulations disentangled by Cassini. J Geophys Res Space Phys. https://doi.org/ 10.1029/2010JA015434
- Larkin T, Keeton W (1976) Bar magnets mask the effect of normal magnetic disturbances on pigeon orientation. J Comp Physiol A 110:227–231. https://doi.org/10.1007/BF00659141
- Malewski S, Begall S, Burda H, Fusani L (2018) Learned and spontaneous magnetosensitive behaviour in the Roborovski hamster (*Phodopus roborovskii*). Ethology 124(6):423–431. https://doi.org/10.1111/eth.12744
- Malkemper EP, Eder SHK, Begall S, Phillips JB, Winklhofer M, Hart V, Burda H (2015) Magnetoreception in the wood mouse (*Apodemus sylvaticus*): influence of weak frequency-modulated radio frequency fields. Sci Rep 5:9917. https://doi.org/10.1038/srep09917
- Marinissen EJ, Lee DY, Hayes JP, Sellathamby C, Moore B, Slupsky S, Pujol L (2009) Contactless testing: possibility or pipe-dream? In: Design, Automation and Test in Europe Conference and Exhibition, 2009. pp 676–681. https://doi.org/10.1109/DATE.2009. 5090751
- Nießner C, Winklhofer M (2017) Radical-pair-based magnetoreception in birds: radio-frequency experiments and the role of cryptochrome. J Comp Physiol A 203(6):499–507. https://doi.org/10.1007/s00359-017-1189-1
- Pakala WE, Chartier VL (1971) Radio Noise Measurements on Overhead Power Lines from 2.4 to 800 KV. IEEE Transactions on Power Apparatus and Systems. PAS-90 3:1155–1165. https://doi.org/10.1109/TPAS.1971.292880
- Pakhomov A, Bojarinova J, Cherbunin R, Chetverikova R, Grigoryev PS, Kavokin K, Kobylkov D, Lubkovskaja R, Chernetsov N (2017) Very weak oscillating magnetic field disrupts the magnetic compass of songbird migrants. J R Soc Interface. https://doi.org/ 10.1098/rsif.2017.0364
- Pan W, Li K (2014) Atmospheric noises in super low frequency / extremely low frequency ranges. In: Propagation of super low frequency /extremely low frequency electromagnetic waves. Advanced topics in science and technology in China. Springer, Berlin Heidelberg, pp 253–262. https://doi.org/10.1007/978-3-642-39050-0\_8
- Pederick LH, Cervera MA (2016) A directional High Frequency noise model: calibration and validation in the Australian region. Radio Sci 51(1):25–39. https://doi.org/10.1002/2015rs005842
- Phillips JB, Youmans PW, Muheim R, Sloan KA, Landler L, Painter MS, Anderson CR (2013) Rapid learning of magnetic compass direction by C57BL/6 mice in a 4-armed "plus" water maze. PLoS One 8(8):e73112. https://doi.org/10.1371/journal.pone.0073112
- Pinzon-Rodriguez A, Muheim R (2017) Zebra finches have a light-dependent magnetic compass similar to migratory birds. J Exp Biol 220(Pt 7):1202–1209. https://doi.org/10.1242/jeb.148098
- Poole I (2003) 2—Radio waves and propagation. In: Poole I (ed) Newnes guide to radio and communications technology. Newnes, Oxford, pp 17–50. https://doi.org/10.1016/B978-075065612-2/ 50002-0
- Ritz T, Thalau P, Phillips JB, Wiltschko R, Wiltschko W (2004) Resonance effects indicate a radical-pair mechanism for avian magnetic compass. Nature 429(6988):177–180. https://doi.org/10.1038/nature02534



- Ritz T, Wiltschko R, Hore PJ, Rodgers CT, Stapput K, Thalau P, Timmel CR, Wiltschko W (2009) Magnetic compass of birds is based on a molecule with optimal directional sensitivity. Biophys J 96(8):3451–3457. https://doi.org/10.1016/j.bpj.2008.11.072
- Rozhok A (2008) Orientation and navigation in vertebrates. Springer, Berlin. https://doi.org/10.1007/978-3-540-78719-8
- Schiffner I, Wiltschko R (2011) Temporal fluctuations of the geomagnetic field affect pigeons' entire homing flight. J Comp Physiol A 197(7):765–772. https://doi.org/10.1007/s00359-011-0640-y
- Schwarze S, Schneider NL, Reichl T, Dreyer D, Lefeldt N, Engels S, Baker N, Hore PJ, Mouritsen H (2016) Weak broadband electromagnetic fields are more disruptive to magnetic compass orientation in a night-migratory songbird (*Erithacus rubecula*) than strong narrow-band fields. Front Behav Neurosci 10:55. https:// doi.org/10.3389/fnbeh.2016.00055
- Shubin VN, Deminov MG (2019) Global Dynamic Model of Critical Frequency of the Ionospheric F2 Layer. Geomag Aeron 59(4):429–440. https://doi.org/10.1134/S0016793219040157
- Sunspot number and long-term solar observations, royal observatory of Belgium. SILO World Data Center. http://www.sidc.be/SILSO/.
- Thalau P, Ritz T, Stapput K, Wiltschko R, Wiltschko W (2005) Magnetic compass orientation of migratory birds in the presence of a 1.315 MHz oscillating field. Naturwissenschaften 92(2):86–90. https://doi.org/10.1007/s00114-004-0595-8
- Tomanova K, Vacha M (2016) The magnetic orientation of the Antarctic amphipod *Gondogeneia antarctica* is cancelled by very weak radiofrequency fields. J Exp Biol 219(Pt 11):1717–1724. https://doi.org/10.1242/jeb.132878
- Vacha M, Puzova T, Kvicalova M (2009) Radio frequency magnetic fields disrupt magnetoreception in American cockroach. J Exp Biol 212(Pt 21):3473–3477. https://doi.org/10.1242/jeb.028670

- Vanselow KH, Ricklefs K (2005) Are solar activity and sperm whale *Physeter macrocephalus* strandings around the North Sea related? J Sea Res 53(4):319–327. https://doi.org/10.1016/j.seares.2004.
- Volland H (1995) Handbook of atmospheric electrodynamics. CRC Press, Boca Raton, Boca Raton. https://doi.org/10.1201/97802 03719503
- Ward BD, Golley MG (1991) Solar cycle variations in atmospheric noise at High Frequency. In: 1991 Fifth International Conference on HF Radio Systems and Techniques, 22–25, pp 327–331
- Wiltschko R, Thalau P, Gehring D, Niessner C, Ritz T, Wiltschko W (2015) Magnetoreception in birds: the effect of radio-frequency fields. J R Soc Interface. https://doi.org/10.1098/rsif.2014.1103
- Winklhofer M (2004) Vom magnetischen Bakterium zur Brieftaube: geo-Biomagnetismus. Phys Unserer Zeit 35(3):120–127. https://doi.org/10.1002/piuz.200401039
- Yeagley HL (1951) A preliminary study of a physical basis of bird navigation. Part II. J Appl Phys 22(6):746–760. https://doi.org/ 10.1063/1.1700043
- Zarka P, Bougeret JL, Briand C, Cecconi B, Falcke H, Girard J, Grießmeier JM, Hess S, Klein-Wolt M, Konovalenko A, Lamy L, Mimoun D, Aminaei A (2012) Planetary and exoplanetary low frequency radio observations from the Moon. Planet Space Sci 74(1):156–166. https://doi.org/10.1016/j.pss.2012.08.004

**Publisher's Note** Springer Nature remains neutral with regard to jurisdictional claims in published maps and institutional affiliations.

